

Electrochemical Properties of Adriamycin Adsorbed on a Mercury Electrode Surface

Kenji KANO, Tomonori KONSE, Naomi NISHIMURA, and Tanekazu KUBOTA*

Gifu Pharmaceutical University, 6-1 Mitahora-higashi 5-chome, Gifu 502

(Received January 26, 1984)

The electrochemical behavior of adriamycin has been studied by means of cyclic d.c. and a.c. voltammetry with a hanging mercury drop electrode, quinizarin being used as a model compound. Both adriamycin and quinizarin are strongly adsorbed on the mercury electrode with their aromatic ring planes oriented parallel to the electrode surface, and give two sets of reduction waves. The first wave, due to the quinone moieties of the adsorbed adriamycin and quinizarin, has been explained on terms of a two-step one-electron surface redox reaction. The formal standard redox potentials, semiquinone formation constants, and charge transfer rate constants of the surface redox reaction of the quinone moieties have been determined. Although the reduced form of adriamycin is not very stable chemically, it is converted to a stable and electrochemically active form for a few minutes at pH 4.54. The second wave appearing at more negative potential would be due to a kinetic or catalytic process.

Adriamycin, a member of the anthracycline antibiotics, is a highly effective antineoplastic agent.¹⁾ The antitumor properties of the anthracyclines correlate in many case with the ability to cause the intercalative inhibition of DNA temperate functions.^{1,2)} Some other mechanisms, such as the generation of free radical intermediates³⁾ and a bioreductive covalent attachment to DNA,⁴⁾ have been suggested. Serious disadvantages of this drug are the cardiotoxicity⁵⁾ and chromosomal damage,⁶⁾ which have been shown to be associated with the inhibition of mitochondrial electron transport to bring about the generation of hydrogen peroxide, superoxide anion, and hydroxyl radicals.⁷⁾ This behavior should be in intimate correlation with the redox properties of the drugs, which then have been the subject of intensive studies.^{3,8–10)}

Rao *et al.*⁸⁾ have investigated the electrochemical reduction behavior of daunomycin and adriamycin. They reported two sets of reduction waves. Since their experiments were carried out at quite a high concentration by using a hanging mercury electrode, the waves reported by them seem to be attributable to the redox systems of both the adsorbed and bulk species, and the analysis of the results has been semi-quantitative. The electrochemical behavior of adsorbed adriamycin has been also reported by Molinier-Jumel *et al.*⁹⁾ on the reduction at a mercury electrode, and by Baldwin *et al.*^{10a)} and Chaney and Baldwin^{10b)} on the oxidation at a carbon paste electrode. Their analyses of the electrochemical behavior of adsorbed adriamycin have, however, remained qualitative.

Recently Kakutani and Senda¹¹⁾ have presented the theory of d.c. and a.c. voltammetry for a two-step surface redox reaction. This theory has been successfully applied to explain the electrochemical behavior of adsorbed flavin mononucleotide,¹²⁾ flavin adenine dinucleotide,¹³⁾ and glucose oxidase.¹⁴⁾ In this study, we have investigated the electrochemical behavior of adriamycin adsorbed on a hanging mercury drop electrode by means of cyclic d.c. and a.c. voltammetry, quinizarin being used as a model compound. The wave ascribed to the quinone moiety of the adsorbed adriamycin has been interpreted by applying the above theory of the two-step surface redox reaction. The

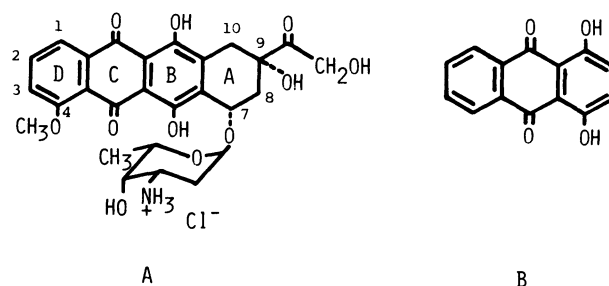


Fig. 1. Structure of adriamycin (A) and quinizarin (B).

thermodynamic and kinetic properties of the electrochemical redox reaction of the adsorbed adriamycin were able to be determined. We have also investigated the second wave, which appeared at a more negative potential than in the quinone wave. The results and discussions are presented in this paper.

Experimental

Chemicals. Adriamycin hydrochloride, obtained from Kyowa Hakko Kogyo Co., was used as received. The concentration of adriamycin in methanol solution was determined spectrophotometrically using $E_{1\text{cm}}^{1\%}(495\text{ nm})=223$.¹⁰⁾ Quinizarin (1,4-dihydroxyanthraquinone), obtained from Ardrich Chemical Co., was purified by recrystallization from methanol. Its purity was checked by elemental analysis. Triply distilled water was used to prepare the electrolysis solution. Other chemicals were reagent grade quality.

Electrochemical Measurements. Cyclic d.c. voltammograms were recorded with a Yanagimoto P-1000 voltammetric analyzer, equipped with a Watanabe WX-4401 X-Y recorder. The a.c. voltammetric measurements were performed with a NF circuit LI-572B lock-in amplifier, equipped with the above potentiostat system. The NF circuit FG-121B function generator was used as an a.c. signal generator.

All the voltammetric measurements were made under potentiostatic conditions with a three-electrode system consisting of a Metrohm EA 290 hanging mercury drop working electrode (HMDE) with surface area $0.0187 \pm 0.0003\text{ cm}^2$, a coiled platinum wire auxiliary electrode, and a Yanagimoto MR-P2 saturated calomel reference electrode (SCE). The buffer solutions of 0.2 mol dm^{-3} sodium acetate-acetic acid were used as the base solution for pH 2 to 6. The ionic strength of the base solutions was adjusted to 0.5 mol dm^{-3}

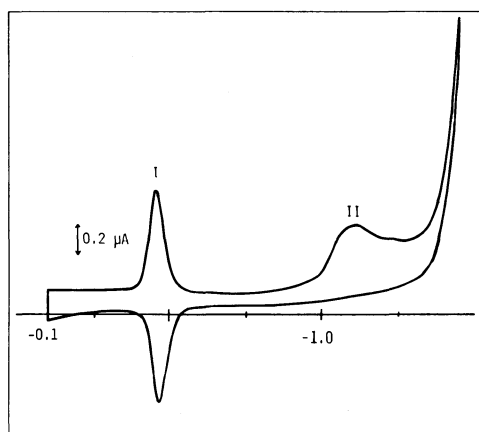
with potassium nitrate. A fresh mercury drop from the HMDE was exposed to the electrolysis solution for a given period of time, t_{exp} , at a constant d.c. potential, E_i . Then the d.c. voltage scan was started from E_i , with the scan rate $v=100 \text{ mV s}^{-1}$ for d.c. voltammetry and with $v=10 \text{ mV s}^{-1}$ for a.c. voltammetry, unless otherwise stated. In a.c. voltammetry, the amplitude of the superimposed a.c. voltage was adjusted to 10 mV peak to peak. The frequency and the amplitude of the a.c. signal were checked with a Iwatsu SS-5702 synchroscope. Electrochemical measurements were performed under nitrogen or argon atmosphere at $25.0 \pm 0.2^\circ \text{C}$, unless otherwise noted.

Results

1. Electrochemical Behavior of Adriamycin.

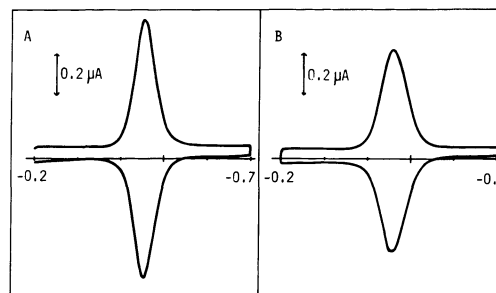
Figure 2 shows the cyclic d.c. voltammogram of $3.75 \times 10^{-6} \text{ mol dm}^{-3}$ adriamycin in a pH 4.54 acetate buffer, which was recorded after $t_{\text{exp}}=3 \text{ min}$ at $E_i=-0.1 \text{ V}$. At such a low concentration, the current due to the redox reaction of diffusing adriamycin will be negligibly small compared with the current due to the surface redox reaction of adsorbed adriamycin. One-pair of the peak-shaped cathodic and anodic waves (I) and one irreversible cathodic wave (II) were observed at -0.45 V and -1.13 V , respectively. For the I waves, the peak potential of the anodic wave is negative by 10 mV compared with that of the cathodic one. We have studied in detail the electrochemical behavior of the I waves, which should be ascribed to the redox reaction of the quinone moiety of adriamycin adsorbed on the HMDE.

Cyclic D.c. Voltammetry of Wave I. Figure 3A shows the cyclic d.c. voltammogram of $1.46 \times 10^{-6} \text{ mol dm}^{-3}$ adriamycin at pH 4.54, which was recorded after $t_{\text{exp}}=4 \text{ min}$ at $E_i=-0.2 \text{ V}$ and with the switching potential, $E_s=-0.7 \text{ V}$. A pair of cathodic and anodic waves are observed at -0.450 V . The shapes and heights of these two waves are practically identical except for the opposite current sign. The peak potential, $E_{p,I}$, and the half-peak width of the wave I, $\Delta E_{p/2,I}^{\text{dc}}$, are -0.450 V and 52 mV , respectively. Figure 3B shows the cyclic



E/V vs. SCE

Fig. 2. Cyclic d.c. voltammogram of $3.75 \times 10^{-6} \text{ mol dm}^{-3}$ adriamycin in pH 4.54 acetate buffer. $t_{\text{exp}}=3 \text{ min}$ at $E_i=-0.1 \text{ V}$.



E/V vs. SCE

Fig. 3. Cyclic d.c. voltammograms of $1.46 \times 10^{-6} \text{ mol dm}^{-3}$ adriamycin in pH 4.54 acetate buffer. Voltage scan was started after $t_{\text{exp}}=4 \text{ min}$ from (A) $E_i=-0.2 \text{ V}$ and (B) $E_i=-0.7 \text{ V}$.

voltammogram recorded with $E_i=-0.7 \text{ V}$, where adriamycin is adsorbed in a reduced state. As in the case of Fig. 3A, a symmetrical pair of anodic and cathodic waves is observed. However, $E_{p,I}$ of the waves in Fig. 3B is more negative by 8 mV and $\Delta E_{p/2,I}^{\text{dc}}$ is larger by 18 mV compared with those of the waves in Fig. 3A.

We performed the multicyclic voltammetry in the potential range of -0.3 to -0.7 V , with $t_{\text{exp}}=10 \text{ min}$ at $7.98 \times 10^{-7} \text{ mol dm}^{-3}$ adriamycin. In the multicyclic voltammetry with $E_i=-0.3 \text{ V}$ and $E_s=-0.7 \text{ V}$, $E_{p,I}$ shifts cathodic and the peak becomes broad and reshaped as the number of cycles is increased, and in about the 40th cycle the wave reaches a steady state, where $E_{p,I}=-0.483 \text{ V}$ and $\Delta E_{p/2,I}^{\text{dc}}=65 \text{ mV}$. On the other hand, in the multicyclic voltammetry with $E_i=-0.7 \text{ V}$ and $E_s=-0.3 \text{ V}$, $E_{p,I}=-0.476 \text{ V}$, and $\Delta E_{p/2,I}^{\text{dc}}=73 \text{ mV}$ for the first scan, and $E_{p,I}$ shifts cathodic and the peak becomes sharp with the increasing number of cycles. In about the 20th cycle, the wave reaches a steady state; this coincides with the steady state wave obtained in the multicyclic voltammetry with $E_i=-0.3 \text{ V}$. These results can be interpreted as follows. The parent compound is fundamentally d.c. reversible and the peak potential is -0.450 V as written above, but the reduced form is chemically not so stable and transferred into a chemically stable other form during the time in which adriamycin was in the reduced form. The chemically stable product is also electrochemically active and shows a d.c. reversible wave, whose peak potential is -0.483 V .

In the following, we have set the E_i at a more positive potential than the peak potential by at least 150 mV. Figure 4 shows the t_{exp} dependence of the cathodic peak height, $I_{p,Ic}$, obtained with $E_i=-0.2 \text{ V}$. At lower concentrations of adriamycin, $I_{p,Ic}$ is proportional to $[(D/r)t_{\text{exp}} + 2(D/\pi)^{1/2}t_{\text{exp}}^{1/2}]$, where D is the diffusion coefficient of adriamycin, estimated by the Ilkovic equation to be $7.53 \times 10^{-6} \text{ cm}^2 \text{ s}^{-1}$, and r is the radius of the HMDE ($3.82 \times 10^{-2} \text{ cm}$ in this case). The slope of the plot is also proportional to the bulk concentration of adriamycin. These results indicate the diffusion-controlled adsorption of adriamycin at the spherical electrode surface, i.e. at the HMDE surface.^{12,16,17} The wave heights reached to a certain limit, $I_{p,Ic}^{\text{max}}$, at the relatively high concentration of adriamycin and/or

prolonged exposure of the HMDE.

Table 1 summarizes the peak heights ($I_{p,lc}$ and $I_{p,la}$), the peak potentials ($E_{p,lc}^{dc}$ and $E_{p,la}^{dc}$), the half-peak widths ($\Delta E_{p/2,lc}^{dc}$ and $\Delta E_{p/2,la}^{dc}$), and the integrated currents *i.e.* the electricities (Q_{lc} and Q_{la}) of the cathodic and anodic waves with various ν . The values of Q_{lc} and Q_{la} were estimated from the area under the wave. Both $I_{p,lc}$ and $I_{p,la}$ are proportional to ν . The $I_{p,lc}/I_{p,la}$ ratio is practically unity. $E_{p,lc}^{dc}$ and $E_{p,la}^{dc}$, $\Delta E_{p/2,lc}^{dc}$ and $\Delta E_{p/2,la}^{dc}$, and Q_{lc} and Q_{la} coincide with each other and are independent of ν . Further, $I_{p,lc}$ and $I_{p,la}$ are proportional to Q_{lc} and Q_{la} , respectively, as shown in Fig. 5. This means that the peak height at a given ν is directly proportional to the amount of the adriamycin adsorbed on the electrode surface. These results indicate that the I wave can be ascribed to the reversible surface redox reaction under the limited conditions, where the effect of the following chemical reaction can be disregarded.

At lower pH than 6, the behavior of the cyclic d.c. voltammograms of adriamycin fundamentally resembles that of the voltammograms obtained at pH 4.54, except for the peak potential. The pH dependence of the peak potential is -60 mV per pH unit in the pH range of 2 to 6, which indicates two-electron two-proton redox reaction.

A.c. Voltammetry of Wave I. In the cyclic a.c. voltammetry of adriamycin adsorbed at $E_i = -0.30$ V and pH 4.54, the a.c. cathodic voltammogram is practically identical in height and shape with the anodic one. So,

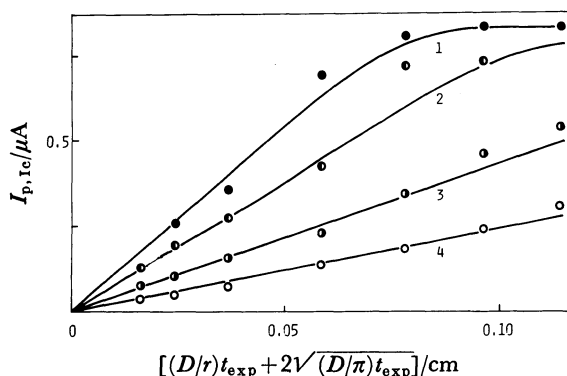


Fig. 4. Dependence of $I_{p,lc}$ on t_{exp} at $E_i = -0.2$ V in pH 4.54 acetate buffer containing adriamycin at (1) 2.19×10^{-6} mol dm $^{-3}$, (2) 1.46×10^{-6} mol dm $^{-3}$, (3) 7.30×10^{-7} mol dm $^{-3}$, and (4) 3.65×10^{-7} mol dm $^{-3}$.

the a.c. voltammetric behavior has been studied only for the cathodic scan. Figure 6 shows the a.c. voltammograms recorded with a.c. frequency, f , of 100 Hz after

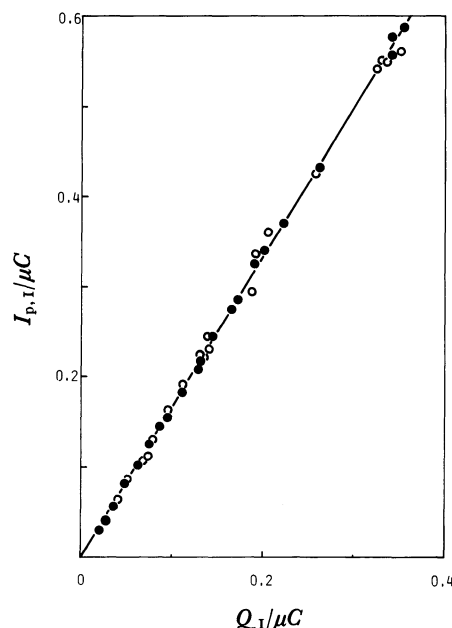


Fig. 5. Plot of the peak current against the electricity at pH 4.54. The closed and open circles correspond to the cathodic and anodic waves, respectively. $E_i = -0.2$ V.

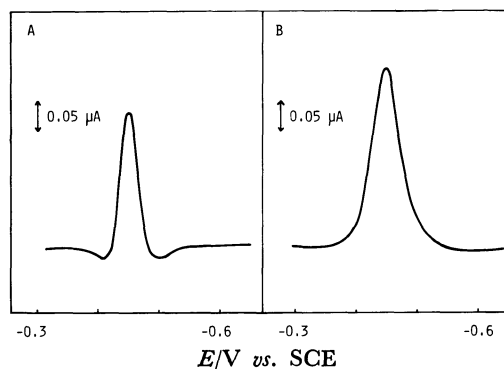


Fig. 6. A.c. voltammograms of 2.16×10^{-6} mol dm $^{-3}$ adriamycin in pH 4.54 acetate buffer at 100 Hz. $t_{exp} = 2$ min at $E_i = -0.30$ V. (A) Real component, (B) imaginary component.

TABLE 1. SCAN-RATE DEPENDENCE OF THE PEAK CURRENT, PEAK POTENTIAL, HALF-PEAK WIDTH, AND INTEGRATED CURRENT OF d.c. VOLTAMMOGRAM OF ADRIAMYCIN ADSORBED ON A MERCURY ELECTRODE AT pH 4.54^{a)}

Scan rate mV s $^{-1}$	$I_{p,lc}$ μA	$I_{p,la}$ μA	$E_{p,lc}^{dc}$ V vs. SCE	$E_{p,la}^{dc}$ V vs. SCE	$\Delta E_{p/2,lc}^{dc}$ mV	$\Delta E_{p/2,la}^{dc}$ mV	Q_{lc} μC	Q_{la} μC
20	0.086	0.085	-0.453	-0.454	52	52	0.211	0.213
50	0.188	0.186	-0.451	-0.451	52	52	0.211	0.212
100	0.348	0.347	-0.450	-0.452	52	52	0.212	0.210
200	0.649	0.648	-0.450	-0.453	52	52	0.209	0.210
500	1.705	1.700	-0.450	-0.451	53	53	0.211	0.211

a) $C_{adriamycin} = 1.46 \times 10^{-6}$ mol dm $^{-3}$, $t_{exp} = 2$ min at $E_i = -0.2$ V.

TABLE 2. PEAK POTENTIAL AND HALF-PEAK WIDTH OF a.c. VOLTAMMOGRAM OF ADRIAMYCIN ADSORBED ON A MERCURY ELECTRODE AT pH 4.54^{a)}

Frequency Hz	E_p^{real}	E_p^{imag}	$\Delta E_{p/2}^{\text{real}}/\text{mV}$		$\Delta E_{p/2}^{\text{imag}}/\text{mV}$	
	V vs. SCE		Obsd	Calcd ^{b)}	Obsd	Calcd ^{b)}
100	-0.450	-0.450	37	42.0	50	52.4
200	-0.449	-0.453	40	42.4	53	53.2
300	-0.450	-0.448	41	43.1	55	54.5
400	-0.448	-0.450	45	44.0	57	56.2
500	-0.450	-0.450	45	45.1	60	58.2

a) $C_{\text{adriamycin}} = 1.13 \times 10^{-6} \text{ mol dm}^{-3}$, $t_{\text{exp}} = 3 \text{ min}$ at $E_i = -0.3 \text{ V vs. SCE}$. b) Calculated by using $K = 0.132$, $k_{\text{sap}} = 8.80 \times 10^3 \text{ s}^{-1}$, and $\theta = 0.392$.

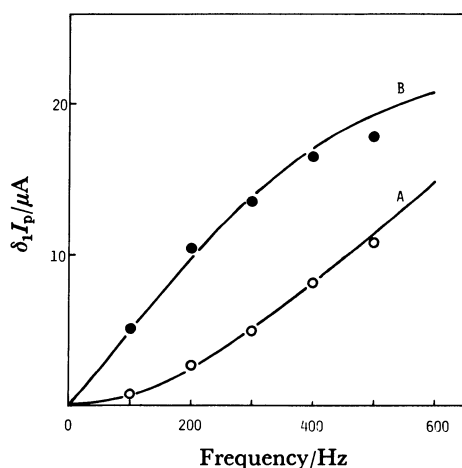


Fig. 7. Dependence of (A) δI_p^{real} and (B) δI_p^{imag} on a.c. frequency. A.c. voltammograms were recorded in pH 4.54 acetate buffer containing $1.13 \times 10^{-6} \text{ mol dm}^{-3}$ adriamycin after $t_{\text{exp}} = 2 \text{ min}$ at $E_i = -0.30 \text{ V}$. Solid lines represent theoretical curves¹¹⁾ calculated by using $K = 0.132$, $k_{\text{sap}} = 8.8 \times 10^3 \text{ s}^{-1}$, and $\Gamma = 4.04 \times 10^{-11} \text{ mol cm}^{-2}$ ($\theta = 0.392$).

$t_{\text{exp}} = 2 \text{ min}$ at $E_i = -0.3 \text{ V}$ in the pH 4.54 acetate buffer containing $2.16 \times 10^{-6} \text{ mol dm}^{-3}$ adriamycin. In all the a.c. voltammograms recorded in this study, the peak potentials of the real and the imaginary components, E_p^{real} and E_p^{imag} , are independent of the a.c. frequency between 100 and 500 Hz, and of the amount of the adsorbed adriamycin. They are also in accord with each other, and with the peak potentials of the corresponding d.c. voltammogram, as shown in Table 2. On the other hand, the peak currents, δI_p^{real} and δI_p^{imag} , and the half-peak widths, $\Delta E_{p/2}^{\text{real}}$ and $\Delta E_{p/2}^{\text{imag}}$, of the real and imaginary components depend on f and on the amount of the adsorbed adriamycin, as shown in Fig. 7 and Table 2.

D.c. Voltammetry of Wave II. We have also studied the d.c. voltammetric behavior of the irreversible cathodic wave II, observed at -1.13 V with $\nu = 100 \text{ mV s}^{-1}$ in a pH 4.54 acetate buffer. The peak potential of the wave II shifts cathodic by about 50 mV for the tenfold increase in the ν range of 10 to 500 mV s^{-1} . The peak current of the II wave, $I_{p,II}$, grows parabolically with increasing ν ; here $I_{p,II}$ was obtained by subtracting the current of the base solution without adriamycin. Figure 8 shows the ν dependence of the

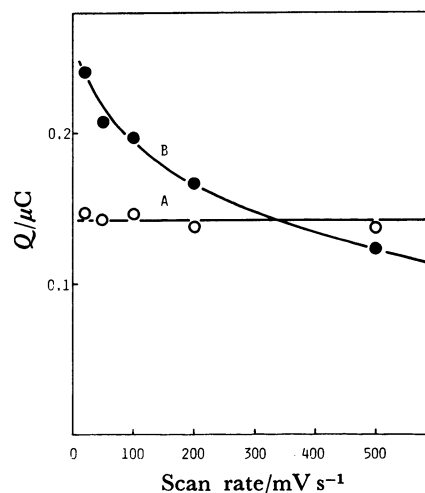


Fig. 8. Dependence of (A) Q_{Ic} and (B) Q_{II} on the scan rate in pH 4.54 acetate buffer containing $9.97 \times 10^{-7} \text{ mol dm}^{-3}$ adriamycin. D.c. voltammograms were recorded after $t_{\text{exp}} = 3 \text{ min}$ at $E_i = -0.10 \text{ V}$.

integrated current of the II wave, Q_{II} , as well as that of the cathodic wave I, Q_{Ic} , where the voltammograms were recorded with $E_i = -0.1 \text{ V}$, and t_{exp} was set to be 3 min, which included the potential scanning time from E_i to the peak potential of wave II. Q_{II} decreases with increasing ν . This coincides with the parabolic ν dependence of $I_{p,II}$. The temperature coefficient of $I_{p,II}$ is 6.3% in the temperature range of 10 to 40°C . These results indicate that wave II is kinetic or catalytic in character.

The current of wave II is reduced with addition of *N,N*-dimethylformamide (DMF). Curve 1 in Fig. 9 shows the dependence of $I_{p,II}$ on the amount of the added DMF. It disappears completely at the DMF concentrations beyond 20% (v/v).

II. Electrochemical Behavior of Quinizarin. Figure 10A shows the cyclic d.c. voltammogram of $3.98 \times 10^{-6} \text{ mol dm}^{-3}$ quinizarin in pH 4.54 acetate buffer. It was recorded after $t_{\text{exp}} = 3 \text{ min}$ at $E_i = -0.1 \text{ V}$. Just like the case of adriamycin, one pair of peak-shaped cathodic and anodic waves (I) and one irreversible cathodic wave (II) are recorded at -0.416 V and -1.095 V , respectively. However, the peak potentials of the cathodic and anodic waves I are in accord with each other, and the anodic peak current is about one-half

of the cathodic one. This I wave should be ascribed to the redox reaction of the quinone moiety of quinizarin adsorbed on the HMDE.

In the case of cyclic d.c. voltammetry starting with $E_i = -0.2$ V and setting the E_s in the potential range of -0.6 to -0.9 V, the shapes and heights of the cathodic and anodic waves become practically identical except for the opposite current sign (Fig. 10 B). $E_{p,1}$ and $\Delta E_{p/2,1}$ of the wave are -0.416 and 53 mV, respectively, at pH 4.54. These values coincide well with those of the wave obtained with $E_i = -0.7$ V and $E_s = -0.2$ V. This kind of behavior of quinizarin is quite different from that of the aforementioned adriamycin, and shows that the reduced quinizarin is stable chemically, but partial desorption occurs at the more negative potential than -1.0 V. Detailed analysis of these waves in d.c. and a.c. voltammetry leads to the conclusion that the electrochemical behavior of wave I given by quinizarin is fundamentally the same as that of the d.c. reversible wave I given by adriamycin. The II wave decreases and disappears as more DMF is added, as shown in Fig. 9 (curve 2).

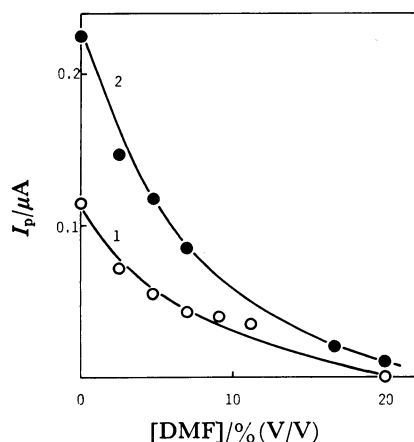


Fig. 9. Dependence of $I_{p,II}$ of (1) adriamycin and (2) quinizarin on the concentration of DMF. $C_{\text{adriamycin}} = 1.25 \times 10^{-6}$ mol dm $^{-3}$, $C_{\text{quinizarin}} = 2.49 \times 10^{-6}$ mol dm $^{-3}$, $t_{\text{exp}} = 3$ min at $E_i = -0.1$ V.

Discussion

Adsorption of Adriamycin on Mercury Electrode Surface. The present study has revealed that adriamycin is strongly adsorbed on the HMDE surface and that the adsorption is controlled by diffusion.

The peak current of the wave I is given by

$$I_p = kA\Gamma = kA[(D/r)t_{\text{exp}} + 2(D/\pi)^{1/2}t_{\text{exp}}^{1/2}]C, \quad (1)$$

where k is the proportional constant, A the electrode surface area, Γ the surface concentration of adriamycin per unit area, and C the bulk concentration of adriamycin. At large C and/or large t_{exp} , the maximum current, I_p^{max} , is obtained, so that the I_p^{max} is given by

$$I_p^{\text{max}} = kA\Gamma^{\text{max}}, \quad (2)$$

where Γ^{max} is the maximum Γ . By applying Eqs. (1) and (2) to such a plot as is shown in Fig. 4, we estimated $\Gamma^{\text{max}} = 1.4 \times 10^{-10}$ mol cm $^{-2}$ at -0.2 V and at pH 4.54. The Γ and Γ^{max} values can also be estimated from the integrated current;

$$Q = nFA\Gamma \text{ and } Q^{\text{max}} = nFA\Gamma^{\text{max}}, \quad (3)$$

where n is the number of electrons transferred per molecule of adriamycin. For the I wave obtained with $E_i = -0.20$ V, this gives $\Gamma^{\text{max}} = 1.1 \times 10^{-10}$ mol cm $^{-2}$ at pH 4.54, by assuming $n=2$ (for the redox of quinone moiety). Further, when adriamycin is adsorbed at $E_i = -0.65$ V, where the reduced adriamycin is adsorbed, Γ^{max} is estimated to be 1.2×10^{-10} mol cm $^{-2}$ by Eqs. (1) and (2), and 1.1×10^{-10} mol cm $^{-2}$ by Eq. (3). The Γ^{max} values thus obtained by two different treatments agree well between the parent and reduced adriamycins, so that the adsorbed state of the reduced adriamycin is essentially the same as that of the parent adriamycin. Assuming that adriamycin is adsorbed on the electrode surface with its aromatic ring plane oriented parallel to the electrode surface and with its sugar moiety perpendicular to the electrode surface, a CPK molecular model¹⁸⁾ gives $\Gamma^{\text{max}} = 1.1 \times 10^{-10}$ mol cm $^{-2}$.

The Γ^{max} value of 1.4×10^{-10} mol cm $^{-2}$ was estimated for quinizarin by the two methods: One is the applica-

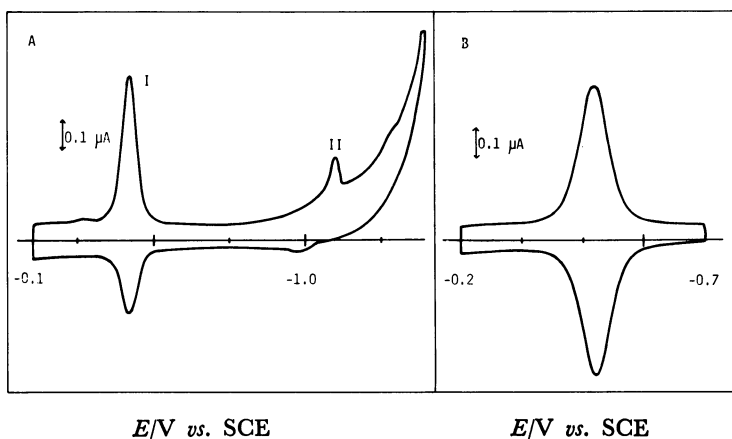
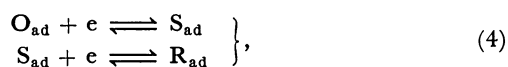


Fig. 10. Cyclic d.c. voltammograms of 3.98×10^{-6} mol dm $^{-3}$ quinizarin in pH 4.54 acetate buffer. $t_{\text{exp}} = 3$ min. (A) $E_i = -0.1$ V and $E_s = -1.4$ V, (B) $E_i = -0.2$ V and $E_s = -0.7$ V.

tion of Eq. (3), and the other is due to the CPK model method, where we assumed parallel orientation of its aromatic ring. The difference between Γ_{\max} of adriamycin and quinizarin can be ascribed to the ring A in adriamycin, which is absent in quinizarin. In other words, the sugar moiety in the adsorbed adriamycin is directly surrounded by the solvent molecules. This conformation of the adsorbed adriamycin may be similar to that of the pyridine adduct of daunomycin in the crystal structure, in which strong hydrogen bonding is formed between the two axial oxygen groups at C₇ and C₉.¹⁹

Surface Redox Process of Quinone Moiety in Adsorbed Adriamycin. The I wave brought about by adriamycin adsorbed on the HMDE surface should be ascribed to the redox reaction of the quinone moiety. This wave is reversible under the conditions that the d.c. voltammogram is recorded with $E_i = -0.2$ V and $E_s = -0.7$ V. As was written in detail in the section "Cyclic Voltammetry of Wave I" in the chapter "Results", the reduced form of adriamycin is not very stable, and is irreversibly transferred into other stable form, which is also capable of a reversible two-electron redox reaction. This chemical reaction would be considered as an irreversible elimination of the amino sugar moiety, giving rise to 7-deoxyadriamycinone, as stated by Rao *et al.*⁹ This proposed process is supported by the fact that adriamycin is quantitatively converted into 7-deoxyaglycon by mild chemical reduction.²⁰ Furthermore, this reductive cleavage process is one important metabolic pathway.²¹

Let us now consider the d.c. reversible wave I produced by the parent adriamycin adsorbed at the more anodic potential side than the peak potential of wave I. The cyclic d.c. voltammetric behavior of wave I should be interpreted in terms of a two-step one-electron surface redox reaction:



where O_{ad}, S_{ad}, and R_{ad} denote the oxidized (or parent), semiquinone and reduced form of the adsorbed adriamycin, respectively. The theory of the cyclic d.c. voltammogram and of the real and imaginary components of the a.c. current in the two-step surface redox reaction has been presented by Kakutani and Senda.¹¹ The theory predicts the following: If the two steps are d.c. reversible in the simplified case²² and the semiquinone formation constant, K , is less than 16, the cathodic and anodic d.c. voltammograms may have a maximum at E'_0 regardless of ν and Γ . Here note that the E'_0 corresponds to the standard surface redox potential of the couple O_{ad}/R_{ad}. Also, the half-peak widths, $\Delta E_{p/2,1c}^{\text{dc}}$ and $\Delta E_{p/2,1a}^{\text{dc}}$, will have the same value and are independent of ν and Γ under the above conditions. Thus Eq. (5) is obtained:

$$\Delta E_{p/2,1c}^{\text{dc}} = \Delta E_{p/2,1a}^{\text{dc}} = (2RT/F) |\ln \zeta|, \quad (5)$$

where ζ is the solution of the equation, $\zeta^4 - K\zeta^3 + (K - 4\sqrt{K} - 6)\zeta^2 - K\zeta + 1 = 0$. The cathodic and anodic peak heights will be proportional to ν and Γ , and are given by

$$\begin{aligned} I_{p,1c} &= I_{p,1a} = 2(F^2/RT)A\Gamma\nu/(2 + \sqrt{K}) \\ &= (F/RT)Q\nu/(2 + \sqrt{K}). \end{aligned} \quad (6)$$

Here K is defined by

$$\begin{aligned} K &= [\text{S}_{\text{ad}}]^2/[\text{O}_{\text{ad}}][\text{R}_{\text{ad}}] \\ &= \exp[(F/RT)(E'_{01} - E'_{02})], \end{aligned} \quad (7)$$

where E'_{01} and E'_{02} are the standard surface redox potentials of the couples O_{ad}/S_{ad} and S_{ad}/R_{ad}, respectively, and other symbols have their common meanings.

All experimental results obtained in this study agree well with these theoretical predictions (see Table 1 and Fig. 5), and $E'_0 = -0.450$ V at pH 4.54. The K value at pH 4.54 has been determined to be 0.138 ± 0.043 by Eq. (5) and 0.126 ± 0.034 by Eq. (6). These agree well with each other.

The theory also leads to the following outcomes under the aforementioned conditions; E_p^{real} and E_p^{imag} will be independent of the a.c. frequency, f , and will coincide with E'_0 . The ratio of $\delta_1 I_p^{\text{real}}$ to $\delta_1 I_p^{\text{imag}}$ at $E = E'_0$ is given by

$$(\delta_1 I_p^{\text{real}}/\delta_1 I_p^{\text{imag}})_{E=E'_0} = 2\pi f/k_{\text{sap}}(K)^{1/4} \quad (8)$$

where k_{sap} is the apparent rate constant of the first and the second charge transfer step. The present result is in line with the prediction discussed hitherto as shown in Table 2 and Fig. 11. The slope of the plot in Fig. 11 gives k_{sap} by applying the K value determined by d.c. voltammetry. The k_{sap} value has been estimated to be $8.8 \times 10^3 \text{ s}^{-1}$ at $\Gamma = 4.04 \times 10^{-11} \text{ mol cm}^{-2}$ ($\theta \equiv \Gamma/\Gamma_{\max} = 0.392$), using $K = 0.132$. According to the theoretical equations in the simplified case, we have calculated the half-peak widths and the peak currents of the real and imaginary components of a.c. voltammogram using the estimated values of K , k_{sap} , and Γ . Table 2 shows the experimental and theoretical values of $\Delta E_{p/2}^{\text{real}}$ and $\Delta E_{p/2}^{\text{imag}}$. Figure 7 shows the f dependence of the experimental values of a.c. peak current, where the solid lines represent the theoretical ones.

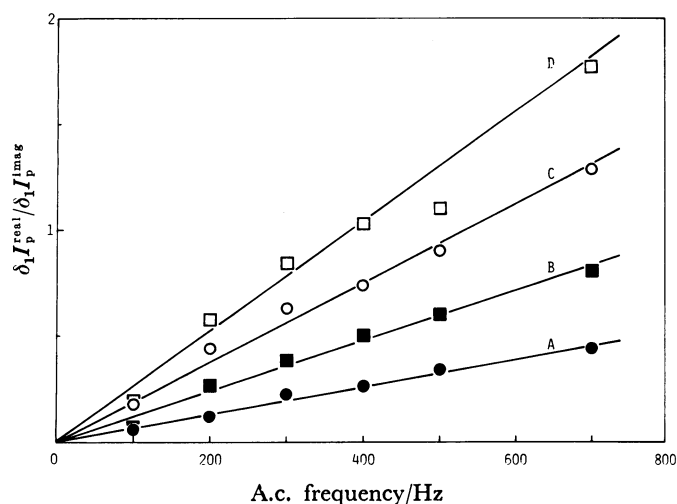


Fig. 11. Dependence of the a.c. peak current ratio, $\delta_1 I_p^{\text{real}}/\delta_1 I_p^{\text{imag}}$, on a.c. frequency at various total surface coverages of adriamycin in pH 4.54 acetate buffer. $\theta =$ (A) 0.19, (B) 0.39, (C) 0.65, and (D) 1.0.

Agreement between the experimental results and the theoretical predictions is good. The dependence of k_{sap} on the surface coverage, θ , is also given by Eq. (9)¹¹⁾

$$k_{\text{sap}} = k_{\text{sap}}(\theta \rightarrow 0) \exp(-a\theta), \quad (9)$$

where $k_{\text{sap}}(\theta \rightarrow 0)$ is the apparent rate constant at $\theta \rightarrow 0$, and a is the Frumkin's a -parameter of interaction between adsorbed molecules (a is positive for attraction and negative for repulsion). This situation is experimentally verified as shown in Fig. 12. From the slope of the plot in Fig. 12, we can estimate the a value. In conclusion, one can say that the cyclic d.c. and a.c. voltammetric behavior of the quinone moiety in the adriamycin adsorbed on the HMDE can be explained by the two-step surface redox mechanism. Now, the E'_{o1} and E'_{o2} values can be estimated by using the E'_o in Eq. (10) and the K in Eq. (7):

$$E'_o = (E'_{o1} + E'_{o2})/2. \quad (10)$$

Table 3 summarizes the above electrochemical data. We have also determined the electrochemical data of the quinone moiety of the adsorbed adriamycin at pH 2.49; these are listed in Table 3. In the range of pH lower than 6, E'_{o1} and E'_{o2} as well as E'_o shift linearly to negative with the slope of -60 mV/pH. This result indicates that each of two steps of the surface redox process involves one electron and one proton. Other electrochemical data obtained at pH 2.69 are practically identical with those obtained at pH 4.54. The electrochemical behavior of adsorbed adriamycin becomes complicated at elevated pH; this will be reported in a succeeding paper.

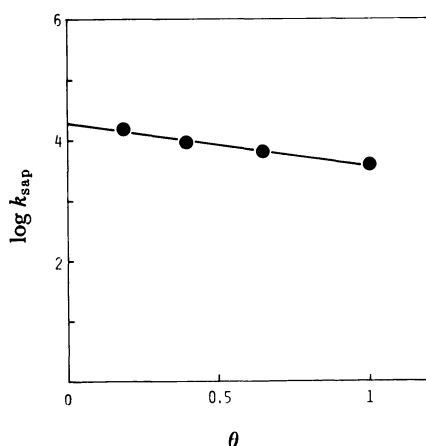


Fig. 12. Plot of $\log k_{\text{sap}}$ of adriamycin against θ at pH 4.54.

Similarly, the electrochemical behavior of the quinone moiety in the adsorbed quinizarin is explained by the above mechanism. The electrochemical data are summarized in Table 3. A decrease in $k_{\text{sap}}(\theta \rightarrow 0)$ and a -parameter is observed for quinizarin, compared with the values for adriamycin. The difference in E'_o between adriamycin and quinizarin is mainly ascribed to 4-methoxyl group of adriamycin. The K values of adriamycin and quinizarin are less than unity, indicating that the disproportionation of the adsorbed semiquinone form should be thermodynamically favorable.

Electrochemical Process in Wave II Produced by Adriamycin.

The d.c. voltammetric behavior of the II wave indicates that the current has a kinetic or catalytic character. The II wave is also observed with quinizarin, but not with anthraquinone.²³⁾ These facts suggest that the presence of two adjacent hydroquinone moieties in a molecule is essential for the appearance of the II wave. Note that the quinone moiety is reduced to the hydroquinone moiety at the potential where the II wave is observed. The process of wave II can thus be ascribed to the catalytic hydrogen evolution current catalyzed by two hydroxyl groups on adjacent benzene rings such as the oxonium compounds.²⁴⁾ The fact that the II wave becomes small and disappears with the addition of DMF, an aprotic solvent, supports the proposed mechanism. Rao *et al.*⁹⁾ have ascribed this irreversible process to the reduction of the side-chain carbonyl group, on the basis of its similarity to the reduction processes of acetophenone and 1'-acetonaphthone. However, the side-chain carbonyl group of adriamycin is aliphatic and is not conjugated with the aromatic rings, differing very much from the carbonyl groups of acetophenone and 1'-acetonaphthone. In general, the reduction wave of aliphatic ketone can not be observed in the usual buffer solution.²⁵⁾ Further, Rao *et al.*'s assignment can not explain the II wave produced by quinizarin, which is without the side-chain carbonyl group.

As a conclusion, the thermodynamic and kinetic information on the redox reaction of adriamycin adsorbed on a mercury electrode surface can be obtained by means of the cyclic d.c. and a.c. voltammetric study. This information would be useful in an elucidation of the action mechanism of adriamycin. The electrochemical behaviors of the adsorbed adriamycin in neutral and alkaline solutions and/or on a solid electrode will be published later.

The authors wish to express their sincere thanks to Professor Mitsugi Senda and Dr. Tadaaki Kakutani, Kyoto University, for their valuable discussions on this study.

TABLE 3. ELECTROCHEMICAL DATA OF ADRIAMYCIN AND QUINIZARIN ADSORBED ON A MERCURY ELECTRODE

Compound	pH	E'_o	E'_{o1}	E'_{o2}	K	$\frac{k_{\text{sap}}(\theta \rightarrow 0)}{10^4 \text{ s}^{-1}}$	a
		V vs. SCE					
adriamycin	4.54	−0.450	−0.476	−0.424	0.132	1.98	1.66
adriamycin	2.69	−0.333	−0.357	−0.308	0.148	2.19	1.61
quinizarin	4.54	−0.418	−0.440	−0.396	0.178	0.73	0.94

References

- 1) A. Di Marco, F. Arcamone, and F. Zunino, "Antibiotics III-Mechanism of Action of Antimicrobial and Antitumor Agents," J. W. Corcoran and F. E. Hahn, eds., Springer, New York (1975), pp. 101–128.
- 2) S. Neidle, "Topics in Antibiotic Chemistry," ed by P. G. Sammes, John Wiley & Sons, New York (1978), Vol. 2, pp. 240–278.
- 3) N. R. Bachur, S. L. Gordon, and M. V. Gee, *Mol. Pharmacol.*, **13**, 901 (1977); L. W. Lown, S. K. Sim, K. C. Majumdar, and R. Y. Chang, *Biochem. Biophys. Res. Commun.*, **76**, 705 (1977); B. Kalynaraman, E. Perez-Reyers, and R. P. Mason, *Biochem. Biophys. Acta*, **630**, 119 (1980); S. Sato, M. Iwaizumi, K. Honda, and Y. Tamura, *Gann*, **68**, 603 (1977); J. W. Lown and H.-H. Chen, *Can. J. Chem.*, **59**, 3212 (1981).
- 4) B. K. Shinha and J. L. Gregory, *Biochem. Pharmacol.*, **30**, 2626 (1981); D. L. Kleyer and T. H. Koch, *J. Am. Chem. Soc.*, **105**, 5154 (1983).
- 5) E. A. Lefrak, J. Pitha, S. Rosenheim, and J. A. Gottlieb, *Cancer*, **32**, 302 (1973); J. P. Rinehart, R. P. Lewis, and S. P. Balcerzak, *Ann. Inter. Med.*, **81**, 475 (1974).
- 6) A. Di Marco, M. Gaetani, P. Orezzi, B. Scarpinato, R. Silvestrini, M. Soldati, T. Dasdia, and L. Valentini, *Nature*, **201**, 706 (1964).
- 7) T. Kishi, T. Watanabe, and K. Folkers, *Proc. Natl. Acad. Sci.*, **73**, 4653 (1976); Y. Iwamoto, I. L. Hansen, T. H. Porter, and K. Folkers, *Biochem. Biophys. Res. Commun.*, **58**, 633 (1974); T. Goodman and P. Hochstein, *Biochem. Biophys. Res. Commun.*, **77**, 797 (1977).
- 8) G. M. Rao, J. W. Lown, and J. A. Plambeck, *J. Electrochem. Soc.*, **125**, 534, 540 (1978).
- 9) C. Molinier-Jumel, B. Malfoy, J. A. Reynaud, and G. Aubel-Sadron, *Biochem. Biophys. Res. Commun.*, **84**, 441 (1978).
- 10) a) R. P. Baldwin, D. Packeff, and T. M. Woodcock, *Anal. Chem.*, **53**, 540 (1981); b) E. N. Chaney, Jr. and R. P. Baldwin, *Anal. Chem.*, **54**, 2556 (1982).
- 11) T. Kakutani and M. Senda, *Bull. Chem. Soc. Jpn.*, **53**, 1942 (1980).
- 12) T. Kakutani, K. Kano, S. Ando, and M. Senda, *Bull. Chem. Soc. Jpn.*, **54**, 884 (1981).
- 13) T. Kakutani, I. Katasho, and M. Senda, *Bull. Chem. Soc. Jpn.*, **56**, 1761 (1983).
- 14) T. Ikeda, S. Ando, and M. Senda, *Bull. Chem. Soc. Jpn.*, **54**, 2189 (1981).
- 15) F. Arcamone, G. Cassinelli, G. Franceschi, S. Penco, C. Pol, S. Redaelli, and A. Selva, "International Symposium on Adriamycin," S. K. Carter, A. Di Marco, M. Ghione, I. N. Krakoff, and G. Mathé eds., Springer Verlag, Berlin (1972), p. 16.
- 16) J. Koryta, *Collect. Czech. Chem. Commun.*, **18**, 206 (1953).
- 17) A. J. Bard and L. R. Faulkner, "Electrochemical Method-Fundamentals and Applications," John Wiley & Sons, New York (1980), p. 145.
- 18) R. A. Harie, "Molecules in Three Dimensions," Am. Soc. of Biol. Chem. Inc., Bethesda, Maryland, U.S.A.
- 19) S. Neidle and G. Taylor, *Biochim. Biophys. Acta*, **479**, 450 (1977).
- 20) T. H. Smith, A. N. Fujiwara, D. W. Henry, and W. W. Lee, *J. Am. Chem. Soc.*, **98**, 1969 (1976).
- 21) V. P. Marshall, E. A. Reisender, L. M. Reineke, J. H. Johnson, and P. F. Wiley, *Biochemistry*, **15**, 4139 (1976); S. Takahashi and N. R. Bachur, *J. Pharmacol. Exptl. Ther.*, **195**, 41 (1975).
- 22) This is the case when $a_{ij}=a$ ($i, j=O_{ad}, S_{ad},$ and R_{ad}), $\alpha_n=\beta_n=0.5$ and $k_{sap}(n)=k_{sap}(n=1, 2)$, where a_{ij} , α_n , β_n , and $k_{sap}(n)$ are Frumkin's interaction parameter between the adsorbed molecules i and j , the cathodic and anodic transfer coefficients, and the apparent rate constant of the n -th charge transfer step, respectively.
- 23) Unpublished result.
- 24) S. G. Mairanovskii, "Catalytic and Kinetic Waves in Polarography," B. M. Fabuss and P. Zuman, translators, Plenum Press, New York (1968), pp. 241–285.
- 25) I. Tachi, "Polarography," (in Japanese), Iwanami, Tokyo (1954), pp. 357–362.